

Multimodality imaging of intermediate lesions: Data from fractional flow reserve, optical coherence tomography, near-infrared spectroscopy-intravascular ultrasound

Dariusz Biały¹, Magdalena Wawrzyńska², Jacek Arkowski², Marcin Rogala³,
Klaudia Proniewska⁴, Wojciech Wańha⁵, Wojciech Wojakowski⁵, Tomasz Roleder^{4,6}

¹Department of Cardiology, Wrocław Medical University, Wrocław, Poland

²Department of Medical Emergencies, Wrocław Medical University, Wrocław, Poland

³St. Jude Medical Company, Poland

⁴KCRI, Krakow, Poland

⁵Third Division of Cardiology, Medical University of Silesia, Katowice, Poland

⁶Department of Cardiology, School of Health Sciences Medical University of Silesia, Katowice, Poland

Abstract

Background: Fractional flow reserve (FFR) assesses a functional impact of the atheroma on the myocardial ischemia, but it does not take into account the morphology of the lesion. Previous optical coherence tomography (OCT), intravascular ultrasound (IVUS) and near-infrared spectroscopy (NIRS) studies presented their potential to detect vulnerable plaques, which is not possible by FFR assessment. With the following study, the intermediate lesions were assessed by FFR, OCT and combined NIRS-IVUS imaging to identify plaque vulnerability.

Methods: Thirteen intermediate lesions were analyzed simultaneously by FFR, OCT and combined NIRS-IVUS imaging.

Results: Two lesions were found to have $FFR \leq 0.80$ (0.65 and 0.76). The other 11 lesions had $FFR > 0.80$ with a mean $FFR 0.88 \pm 0.049$. Two lesions with $FFR \leq 0.80$ had plaque burden (PB) $> 70\%$ and minimal lumen area (MLA) $< 4 \text{ mm}^2$, but neither of these 2 lesions were identified as OCT defined thin fibrous cap atheroma (TCFA), or NIRS-IVUS possible TCFA. Among the other 11 lesions with $FFR > 0.80$, 8 were identified as OCT-defined TCFA, 4 had $PB > 70\%$, 6 had $MLA < 4 \text{ mm}^2$, 2 had both $PB > 70\%$ and $MLA < 4 \text{ mm}^2$, 3 lesions were identified as NIRS-IVUS possible TCFA, and 4 lesions had lipid core burden index > 400 .

Conclusions: The FFR-negative lesions pose traits of vulnerability as assessed simultaneously by IVUS, OCT and NIRS imaging. (Cardiol J 2018; 25, 2: 196–202)

Key words: vulnerable plaque, fractional flow reserve, optical coherence tomography, near-infrared spectroscopy, intravascular ultrasound

Address for correspondence: Tomasz Roleder, MD, PhD, Department of Cardiology, School of Health Sciences Medical University of Silesia in Katowice, ul. Ziołowa 45/47, 40–635 Katowice Poland, tel/fax: +48 32 359 86 04, e-mail: tomaszroleder@gmail.com

Received: 17.02.2017

Accepted: 08.07.2017

Introduction

Fractional flow reserve (FFR) estimation became a standard in the assessment of intermediate lesions. The value of $FFR \leq 0.80$ became a cut-off value to intervene, and such an approach was well documented to reduce the incidences of future major adverse cardiac events (MACE) [1].

Fractional flow reserve assesses a functional impact of atheroma on the myocardial ischemia, but does not take into account the morphology of the lesion. Previous histological and intravascular imaging studies identified features of vulnerable plaques, which are prone to rupture. Post-mortem studies presented that thin fibrous cap atheroma (TCFA) covered rupture plaques [2] and in vivo optical coherence tomography (OCT) identified TCFA more frequently in ST elevation myocardial infarction (STEMI) patients [3]. The prospect study presented that lesions with plaque burden (PB) $\geq 70\%$ and minimal lumen area (MLA) $\leq 4 \text{ mm}^2$ on intravascular ultrasound (IVUS) imaging increased the risk of MACE [4]. A high lipid burden assessed by intravascular near-infrared spectroscopy (NIRS) suggested increased the risk of future MACE [5], and combined NIRS-IVUS imaging study presented its potential to detect TCFA [6].

Given the results of histological and intravascular imaging, the question arose whether FFR assessment was sufficient to exclude intermediate lesions from intervention. With the following study, the intermediate lesion was assessed by the simultaneous OCT and combined NIRS-IVUS imaging together with FFR assessment. The aim of this study was to describe intermediate lesion characteristics in regard to their vulnerability and FFR results.

Methods

Study population

The current study employed intravascular FFR, OCT and combined NIRS-IVUS assessment of identical coronary intermediate lesions of the same patient. All imaging was performed during the same procedure. The study group was selected from patients referred for cardiac catheterization due to chronic stable coronary disease symptoms. Patients with renal failure (creatinine $> 1.5 \text{ mg/dL}$), hemodynamic compromise, contrast allergy, aorto-ostial coronary artery lesions, and calcified lesions were excluded from the study. Intermediate lesions to assess by FFR were selected at the operator's

discretion after the diagnostic angiogram. FFR, OCT, and NIRS-IVUS were performed under heparin anticoagulation (activated clotting time $> 300 \text{ s}$) following intracoronary nitroglycerine ($100\text{--}200 \mu\text{m}$) administration.

NIRS-IVUS and OCT images were analyzed by the independent Core Laboratory (KCRI.org). Also, angiographic quantitative coronary analysis (QCA) was performed. Coronary lesions with incomplete and/or poor quality NIRS-IVUS or OCT scans were removed from the investigation (4 coronary lesions). Hence the ultimate analysis included 14 coronary lesions assessed in 13 patients.

The study was approved by to Local Bioethical Committee of Wrocław Medical University in Poland, and all patients signed an informed consent before the procedure.

QCA measurements

Quantitative coronary analysis was performed offline using a validated CAAS QCA software (Pie Medical Imaging BV) for calculation of minimum lumen diameter and reference lumen diameter (the average of the reference lumen diameter proximal to the lesion and reference lumen diameter distal to the lesion). These data were used to calculate % diameter stenosis [(minimal lumen diameter/reference lumen diameter) $\times 100\%$]. Also, complete coronary segment morphology characteristics were evaluated according to the American Heart Association/American College of Cardiology classification.

FFR measurements

Fractional flow reserve measurements were performed using ILUMIEN™ OPTIS™ PCI Optimization™ System (St. Jude Medical). The adenosine was applied intracoronary to a maximal dose of $140 \mu\text{g}$ for the left coronary artery and $100 \mu\text{g}$ for the right coronary artery. All FFR measurements were performed after the intracoronary injection of nitroglycerine.

OCT image acquisition

The commercially available ILUMIEN™ OPTIS™ PCI Optimization™ System (St. Jude Medical) was used for OCT image acquisition. The tip of the 2.7 Fr. OCT catheter was placed at least 15 mm distally to the imaging target lesion. OCT image acquisition was then performed by the hand injection of contrast (Visipaque; total volume 12–20 mL) and simultaneous OCT catheter pullback at 20 mm/s. Each OCT catheter pullback imaged a total of 54 mm of the vessel.

OCT image analysis

Optical coherence tomography image analysis scrutinized serial cross-sectional images of the vessel, at 1 mm intervals, using the LightLab Imaging Offline Review Station. Plaque composition was analyzed according to previously validated criteria for OCT [7]. In brief, signal rich homogenous plaques were classified as fibrous, signal-poor regions with diffuse borders were classified as lipid and signal-poor regions with well-defined borders were classified as calcified plaques. The magnitude of lipid content was measured as the circumferential extent of lipid in OCT cross-sectional images and expressed in degrees (OCT lipid arc,°).

When lipid arc was stretched > 90°, the OCT lipid-rich plaque was detected. Fibrous cap thickness was derived by measuring the thinnest signal rich zone separating the lipid content from the vessel lumen (μm). The thinnest part of the fibrous cap was measured three times and its average was defined as the fibrous cap thickness. OCT-defined TCFA was defined as a lipid-rich plaque with fibrous cap thickness < 65 μm . Also, the presence of both plaque rupture and/or luminal thrombus was noted during OCT analysis.

The cross-sectional area (CSA), minimum and maximum diameter of the vessel was measured every 1 mm. The smallest CSA in one segment was taken as the OCT-defined minimal CSA. The OCT reference lumen area was estimated as the largest CSA within 10 mm proximally or distally to the minimal lumen CSA in the scanned coronary segment.

Combined NIRS and grey-scale IVUS image acquisition

Combined NIRS and gray-scale IVUS image acquisition was performed using the commercially available TVC Imaging System™ with the 2.4 Fr. TVC Insight Catheter (InfraReDx). The tip of the TVC catheter was positioned at least 10 mm distal to the imaging target lesion. Subsequently, the automated pullback was started with at 0.5 mm/s (240 rotations/min) until the TVC catheter entered the guiding catheter.

NIRS image analysis

The raw spectra of NIRS estimate the probability of the presence of an atherosclerotic lipid core and measurements are displayed as a chemogram — a digit code NIRS map [6]. The NIRS map analysis allows calculation of lipid core burden index (LCBI) in 4 mm pullback compartments.

NIRS map analysis was performed using QIVUS Medis software.

Gray-scale IVUS image analysis

Quantitative gray-scale IVUS measurements were performed every 1 mm in scanned coronary segments using QIVUS Medis software (2.1 version). Cross-sectional images were quantified for lumen CSA, external elastic lamina (EEM) CSA, plaque and media CSA and plaque burden. Plaque and media CSA were calculated as the difference between EEM CSA and lumen CSA. Plaque burden was calculated as plaque and media CSA divided by EEM CSA $\times 100$ (%) at the minimal CSA site.

The IVUS reference lumen area was estimated as the largest CSA within 10 mm located proximally or distally to the minimal lumen CSA in one analyzed coronary segment. The reference EEM CSA was calculated as an average of the proximal and distal EEM CSA with the smallest plaque burden, but not higher than 50%. If either the proximally or distally evaluated plaque burden was $\geq 50\%$, then the proximal or distal EEM CSA with the least plaque burden served as reference.

A lesion was defined as the region between proximal and distal EEM reference sites or as the region between either proximal or distal EEM reference sites or a side branch delimiting the assessed coronary segment. Remodeling index (RI) was calculated by dividing EEM CSA at the site of minimal lumen CSA by reference EEM CSA. Lesions with $\text{RI} \leq 0.95$ were defined as negatively remodeled, while those with an $\text{RI} \geq 1.05$ were defined as positively remodeled. An RI between these values was taken as a non-remodeled vessel.

In every lesion, a lumen vessel volume and EEM volume was calculated based on Simpson's rule (mm^3/cm). These data were used to estimate plaque volume (EEM volume – vessel volume, mm^3/cm) and % plaque volume [$100 \times (\text{plaque volume}) / \text{EEM volume, \%}$].

Co-registration of NIRS, gray-scale IVUS and OCT

During the combined NIRS-IVUS pullback, anatomical landmarks were imprinted on the chemogram and bookmarked on IVUS images — i.e. fiducial points, minimal vessel CSA and side branches. Those landmarks allowed matching of OCT images to corresponding sections of NIRS map, IVUS images, and the coronary angiogram. Such co-registration allowed simultaneous judgment of LCBI values, IVUS measurements and

OCT analysis in the same lesion of the coronary vessel.

The identification of vulnerable lesions

According to the previously published studies, the following vulnerable lesions were identified by OCT and NIRS-IVUS imaging. OCT-defined TCFA as described above, IVUS vulnerable plaque defined as lesion with PB > 70% and MLA < 4 mm² (PROSPECT study) [4], and NIRS-IVUS TCFA described previously as LCBI_{4mm} > 265 with simultaneous positive RI of the vessel [6] and lesions with LCBI_{4mm} > 400, which was the threshold of lipid burden for observed culprit STEMI lesions [8].

Statistical analysis

Kolmogorov-Smirnov analysis assessed the obtained data distribution. For normally distributed values data are presented as mean with standard deviation, for non-normally distributed values data were presented as median with interquartile intervals (IQR, 25 percentile, 75 percentile). Data analysis was performed using Medcalc software (16.8.4).

Results

Patient characteristics

There were 13 patients (8 male; 61%) with stable coronary artery disease enrolled into the study with a mean age 62.84 ± 6.03 years and with a mean body mass index 27.08 ± 2.42. Eleven (85%) patients suffered from hypertension, 6 (46%) had hyperlipidemia, 2 (15%) were diabetic, and 7 (54%) were smokers. All patients received aspirin, 11 (85%) received thienopyridine. Both diabetic patients were using insulin injection.

QCA analysis

The reference lumen diameter was 2.9 (IQR 2.29, 3.39) with MLD 1.44 (IQR 0.96, 1.96) and lesion length 7.06 mm (IQR 6.34, 12.64). The median % DS was 52% (IQR 33, 61). One lesion was classified as B2/C; the other 12 lesions were classified as A/B1.

FFR assessment

Two lesions were found to have FFR < 0.80 (0.65 and 0.76). The other 11 lesions had mean FFR 0.88 ± 0.049. Two FFR positive lesions were located in the proximal and medial segment of the left anterior descending artery (LAD). FFR negative segments were located as follows: 4 in proximal LAD, 4 in medial LAD, 1 in distal left

main, 1 in proximal right coronary artery and 1 in the ramus intermedius. Only FFR positive lesions were stented.

NIRS-IVUS imaging

For the reference segment of the vessel, EEM CSA was 15.59 ± 6.81 mm², lumen CSA was 7.11 ± 3.10 mm², plaque and media CSA was 8.48 ± 3.98 mm², and PB was 53.76 ± 7.69%.

For the minimum lumen site, the EEM CSA was 9.42 mm² (IQR 7.48, 14.53), lumen CSA was 2.75 mm² (IQR 2.35, 4.47), plaque and media CSA was 6.78 mm² (QR 5.02, 10.22), PB was 69.42% (IQR 63.92, 74.96). Plaque volume was 95.42 mm³ (IQR 78.44, 104.28), vessel volume was 155.64 mm³ (IQR 138.94, 194.01), plaque length was 13.46 mm (IQR 7.56, 16.43) and median RI was 1.27 (IQR 1.048, 1.50). Median maxLCBI_{4mm} was 337 (IQR 162, 440).

OCT analysis

Median MLA was 2.62 (IQR 2.25, 4.29), median reference lumen area was 5.85 (IQR 5.49, 8.91) with % area stenosis 57% (IQR 48.65, 65.54). Nine (75%) lesions were calcified with median calcification arc 114 (IQR 104, 153). Ten (83%) lesions were lipid-rich with median lipid arc 172 (IQR 112, 253). Median thickness of the fibrous cap covering the lipid core was 45 μm (IQR 40, 90). Eight lesions were classified as OCT defined-TCFA.

OCT and NIRS-IVUS imaging in detection of plaque vulnerability

Two lesions with FFR ≤ 0.80 had PB > 70% and MLA < 4 mm², but none of these two lesions were identified as OCT defined TCFA or NIRS-IVUS possible TCFA. Among the other 11 lesions with FFR > 0.80, 8 were identified as OCT-defined TCFA, 4 had a PB of more than 70%, 6 had MLA less than 4 mm², 2 had both PB > 70% and MLA < 4 mm², 3 were identified as NIRS-IVUS possible TCFA, and 4 had LCBI > 400 mm (Table 1, Fig. 1).

Discussion

It remains challenging to identify vulnerable plaques which rupture and cause an acute coronary occlusion. Previous intravascular imaging studies focused on morphological patterns of atheroma to detect such lesions, but it did not translate to its identification on daily clinical practice. Furthermore, the introduction of FFR assessment simplified the operator's decision by providing a selection of lesions between those to treat and

Table 1. Comparison of FFR, OCT and NIRS-IVUS imaging and the identification of vulnerable lesion.

| | OCT defined TCFA | PB > 70% | MLA-IVUS < 4 mm ² | PB > 70% and MLA < 4 mm ² | NIRS-IVUS TCFA | LCBI _{4 mm} > 400 |
|---------------------|------------------|----------|------------------------------|--------------------------------------|----------------|----------------------------|
| FFR > 0.80 (n = 11) | 8 (62%) | 4 (31%) | 6 (46%) | 2 (15%) | 3 (31%) | 4 (36%) |
| FFR ≤ 0.80 (n = 2) | 0 (0%) | 2 (15%) | 2 (15%) | 2 (15%) | 0 (0%) | 0 (0%) |

FFR — fractional flow reserve; OCT — optical coherence tomography; TCFA — thin fibrous cap atheroma; PB — plaque burden; MLA — minimal lumen area; IVUS — intravascular ultrasound; NIRS — near-infrared spectroscopy; LCBI_{4 mm} — maximal lipid core burden index in the 4 mm segment

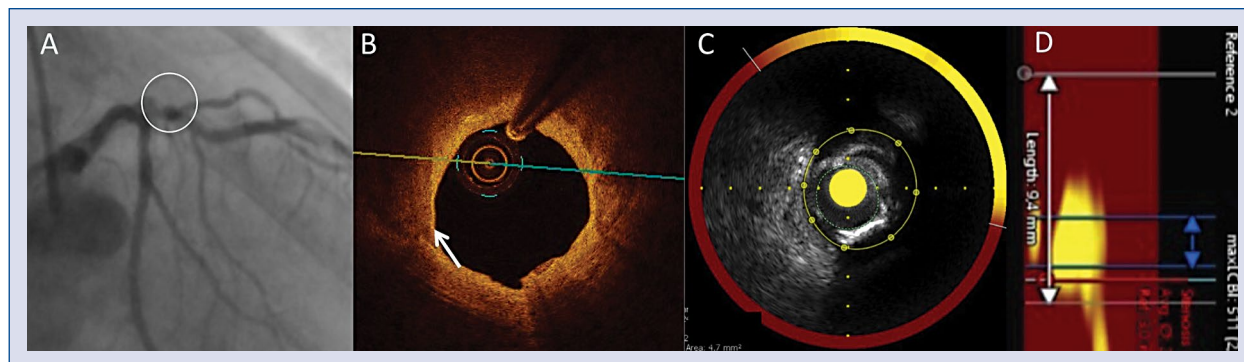


Figure 1. Representative images of fractional flow reserve (FFR) negative lesion by optical coherence tomography (OCT), intravascular ultrasound (IVUS) and near-infrared spectroscopy (NIRS); **A.** The angiography of the intermediate lesion located in the proximal segment of the left descending artery with FFR = 0.87; **B.** OCT presents thin fibrous cap atheroma (white arrow) with minimal lumen area (MLA) = 2.7 mm²; **C.** A combined NIRS-IVUS image presents MLA = 3.6 mm² with plaque burden = 71%; **D.** NIRS map presents the maximal lipid core burden index in 4 mm (LCBI) = 511.

those to be left untouched. Such an approach was strongly indicated by clinical results and significantly improved patient outcome [9, 10]. Nevertheless, it pushed aside lesion morphology assessment, which identifies vulnerable plaques. The presented proof of concept study showed that some of FFR negative lesions still posed traits of vulnerability.

Ischemic lesions increase by 12 times the risk of death at 5 year follow-up [11], and treatment of such lesion decreases MACE [12]. On the other hand, not only lesion functionality increases the risk of future MACE, but lesion morphology as well. Analysis from the PROSPECT study showed that lesions with PB ≥ 70% and MLA ≤ 4 mm² increases 3 times the risk of MACE at 3.4 year follow-up, respectively [4]. The present observations suggested that despite FFR negative results such IVUS vulnerable lesions may remain left untreated and thus, may pose a risk to patients.

Fractional flow reverse positive lesions had more lipids [13], presented higher PB and smaller MLA [14]. Furthermore, the length of the plaque and its volume positively correlated with FFR results as well [15]. Alltogether this suggests that

most of the vulnerable intermediate lesions are already treated based on FFR measurements anyway, but it should be noted that a high consternation of necrotic core was also observed in FFR negative lesions [14]. Clinical observations presented similar clinical outcomes for the coronary lesion discrimination by IVUS or FFR [16], despite the limited utility of IVUS measurements to guide intervention [17]. Similar clinical outcomes for IVUS and FFR guided interventions suggest that some of IVUS guided intervention were preformed in FFR-negative vulnerable lesions, which brought benefit to patients.

Previous OCT analysis presented that non-culprit lesions exposed traits of plaque vulnerability for both acute and stable patients with a higher prevalence of TCFA in obese patients [18, 19]. With the presented study we have also observed OCT-defined TCFA in FFR negative lesions. Such atheroma also prevailed in non-culprit lesions in STEMI patients [3] and was more frequently found in cadavers who died from myocardial infarction [2]. Interestingly, recent studies presented that morphological characteristics of plaques assessed by OCT were not independently associated with

FFR [20]. The presented observation extended these observations and confirmed the presence of OCT-defined TCFA in FFR negative lesions. Therefore, the first prospective COMBINE study has been launched to detect whether OCT-defined TCFA observed in FFR negative lesions of diabetic patients increased the risk of future MACE [21].

Recently, the intravascular NIRS has been introduced into coronary artery assessment, which provides a very simple and quantitative analysis of lipid burden within the assessed lesions. The in vitro study suggested its potential to detect vulnerable plaques [22]. Furthermore, clinical observation advocated that it might identify vulnerable plaques [6, 8] and patients at risk of MACE [5]. Previously NIRS presented a high lipid burden in non-culprit lesions, but the assessment of lesion morphology by NIRS against FFR lesion was not performed previously [23]. With the present study, it was shown that some of the FFR-negative lesions pose traits of vulnerability, as detected by LCBI alone or combined NIRS-IVUS analysis.

This proof of concept study confirmed that 3 leading intravascular modalities might detect different traits of vulnerability in FFR negative lesions, which warrants further observation as to whether such lesions requires intervention. The implantation of drug eluting stent into vulnerable lesions replaces the risk of plaque rupture with risk of in-stent restenosis. Therefore, the concept emerged that TCFA might be covered with bioresorbable vascular scaffold bioresorbable vascular scaffold to thicken the fibrous cap of the lipid-rich plaque and thus to prevent its future rupture [24], but the latest results on bioresorbable vascular scaffold implantation strongly suggests refraining from their reckless use. On the other hand, such lesions may be left untouched and treated conservatively. The application of aggressive lipid-lowering therapy decreased lipid content within the plaque and decreased its vulnerability [25, 26].

Limitations of the study

It was an observational study involving a very small group of patients. Secondly, it mostly referred to FFR-negative lesions, which biased final observations. The lack of patient follow-up limits the strength of the results.

Conclusions

The FFR-negative lesions pose traits of vulnerability as assessed simultaneously by IVUS, OCT and NIRS imaging.

Conflicts of interest: M. Rogala works for St. Jude Medical Poland. T. Roleder is consultant of KCRI.

References

1. Windecker S, Kolh P, Alfonso F, et al. Authors/Task Force members. 2014 ESC/EACTS Guidelines on myocardial revascularization: The Task Force on Myocardial Revascularization of the European Society of Cardiology (ESC) and the European Association for Cardio-Thoracic Surgery (EACTS) Developed with the special contribution of the European Association of Percutaneous Cardiovascular Interventions (EAPCI). *Eur Heart J*. 2014; 35(37): 2541–2619, doi: [10.1093/eurheartj/ehu278](https://doi.org/10.1093/eurheartj/ehu278), indexed in Pubmed: [25173339](https://pubmed.ncbi.nlm.nih.gov/25173339/).
2. Narula J, Nakano M, Virmani R, et al. Histopathologic characteristics of atherosclerotic coronary disease and implications of the findings for the invasive and noninvasive detection of vulnerable plaques. *J Am Coll Cardiol*. 2013; 61(10): 1041–1051, doi: [10.1016/j.jacc.2012.10.054](https://doi.org/10.1016/j.jacc.2012.10.054), indexed in Pubmed: [23473409](https://pubmed.ncbi.nlm.nih.gov/23473409/).
3. Galon MZ, Wang Z, Bezerra HG, et al. Differences determined by optical coherence tomography volumetric analysis in non-culprit lesion morphology and inflammation in ST-segment elevation myocardial infarction and stable angina pectoris patients. *Catheter Cardiovasc Interv*. 2015; 85(4): E108–E115, doi: [10.1002/ccd.25660](https://doi.org/10.1002/ccd.25660), indexed in Pubmed: [25178981](https://pubmed.ncbi.nlm.nih.gov/25178981/).
4. Stone GW, Maehara A, Lansky AJ, et al. PROSPECT Investigators. A prospective natural-history study of coronary atherosclerosis. *N Engl J Med*. 2011; 364(3): 226–235, doi: [10.1056/NEJMoa1002358](https://doi.org/10.1056/NEJMoa1002358), indexed in Pubmed: [21247313](https://pubmed.ncbi.nlm.nih.gov/21247313/).
5. Oemrawsingh RM, Cheng JM, García-García HM, et al. ATHEROREMO-NIRS Investigators. Near-infrared spectroscopy predicts cardiovascular outcome in patients with coronary artery disease. *J Am Coll Cardiol*. 2014; 64(23): 2510–2518, doi: [10.1016/j.jacc.2014.07.998](https://doi.org/10.1016/j.jacc.2014.07.998), indexed in Pubmed: [25500237](https://pubmed.ncbi.nlm.nih.gov/25500237/).
6. Roleder T, Kovacic JC, Ali Z, et al. Combined NIRS and IVUS imaging detects vulnerable plaque using a single catheter system: a head-to-head comparison with OCT. *EuroIntervention*. 2014; 10(3): 303–311, doi: [10.4244/EIJV10I3A53](https://doi.org/10.4244/EIJV10I3A53), indexed in Pubmed: [24769522](https://pubmed.ncbi.nlm.nih.gov/24769522/).
7. Yabushita H, Bouma BE, Houser SL, et al. Characterization of human atherosclerosis by optical coherence tomography. *Circulation*. 2002; 106(13): 1640–1645, indexed in Pubmed: [12270856](https://pubmed.ncbi.nlm.nih.gov/12270856/).
8. Madder RD, Puri R, Muller JE, et al. Confirmation of the Intracoronary Near-Infrared Spectroscopy Threshold of Lipid-Rich Plaques That Underlie ST-Segment-Elevation Myocardial Infarction. *Arterioscler Thromb Vasc Biol*. 2016; 36(5): 1010–1015, doi: [10.1161/ATVBAHA.115.306849](https://doi.org/10.1161/ATVBAHA.115.306849), indexed in Pubmed: [26941016](https://pubmed.ncbi.nlm.nih.gov/26941016/).
9. Barbato E, Toth GG, Johnson NP, et al. A Prospective Natural History Study of Coronary Atherosclerosis Using Fractional Flow Reserve. *J Am Coll Cardiol*. 2016; 68(21): 2247–2255, doi: [10.1016/j.jacc.2016.08.055](https://doi.org/10.1016/j.jacc.2016.08.055), indexed in Pubmed: [27884241](https://pubmed.ncbi.nlm.nih.gov/27884241/).
10. De Bruyne B, Pijls NHJ, Kalesan B, et al. FAME 2 Trial Investigators. Fractional flow reserve-guided PCI versus medical therapy in stable coronary disease. *N Engl J Med*. 2012; 367(11): 991–1001, doi: [10.1056/NEJMoa1205361](https://doi.org/10.1056/NEJMoa1205361), indexed in Pubmed: [22924638](https://pubmed.ncbi.nlm.nih.gov/22924638/).
11. Iskander S, Iskandrian AE. Risk assessment using single-photon emission computed tomographic technetium-99m sestamibi imaging. *J Am Coll Cardiol*. 1998; 32(1): 57–62, indexed in Pubmed: [9669249](https://pubmed.ncbi.nlm.nih.gov/9669249/).
12. Tonino P, Bruyne BDe, Pijls N, et al. Fractional Flow Reserve versus Angiography for Guiding Percutaneous Coronary In-

- tervention. *New England Journal of Medicine*. 2009; 360(3): 213–224, doi: [10.1056/nejmoa0807611](https://doi.org/10.1056/nejmoa0807611).
13. Sakurai S, Takashima H, Waseda K, et al. Influence of plaque characteristics on fractional flow reserve for coronary lesions with intermediate to obstructive stenosis: insights from integrated-backscatter intravascular ultrasound analysis. *Int J Cardiovasc Imaging*. 2015; 31(7): 1295–1301, doi: [10.1007/s10554-015-0699-6](https://doi.org/10.1007/s10554-015-0699-6), indexed in Pubmed: [26129657](https://pubmed.ncbi.nlm.nih.gov/26129657/).
 14. Chung JH, Ann SH, Singh GB, et al. Segmental assessments of coronary plaque morphology and composition by virtual histology intravascular ultrasound and fractional flow reserve. *Int J Cardiovasc Imaging*. 2016; 32(3): 373–380, doi: [10.1007/s10554-015-0794-8](https://doi.org/10.1007/s10554-015-0794-8), indexed in Pubmed: [26498340](https://pubmed.ncbi.nlm.nih.gov/26498340/).
 15. Yang HM, Tahk SJ, Lim HS, et al. Relationship between intravascular ultrasound parameters and fractional flow reserve in intermediate coronary artery stenosis of left anterior descending artery: intravascular ultrasound volumetric analysis. *Catheter Cardiovasc Interv*. 2014; 83(3): 386–394, doi: [10.1002/ccd.25088](https://doi.org/10.1002/ccd.25088), indexed in Pubmed: [23804359](https://pubmed.ncbi.nlm.nih.gov/23804359/).
 16. de la Torre Hernandez JM, Lopez-Palop R, Garcia Camarero T, et al. Clinical outcomes after intravascular ultrasound and fractional flow reserve assessment of intermediate coronary lesions. Propensity score matching of large cohorts from two institutions with a differential approach. *EuroIntervention*. 2013; 9(7): 824–830, doi: [10.4244/EIJV9I7A136](https://doi.org/10.4244/EIJV9I7A136), indexed in Pubmed: [23685248](https://pubmed.ncbi.nlm.nih.gov/23685248/).
 17. Waksman R, Legutko J, Singh J, et al. FIRST: Fractional Flow Reserve and Intravascular Ultrasound Relationship Study. *J Am Coll Cardiol*. 2013; 61(9): 917–923, doi: [10.1016/j.jacc.2012.12.012](https://doi.org/10.1016/j.jacc.2012.12.012), indexed in Pubmed: [23352786](https://pubmed.ncbi.nlm.nih.gov/23352786/).
 18. Maejima N, Hibi K, Saka K, et al. Morphological features of non-culprit plaques on optical coherence tomography and integrated backscatter intravascular ultrasound in patients with acute coronary syndromes. *Eur Heart J Cardiovasc Imaging*. 2015; 16(2): 190–197, doi: [10.1093/ehjci/jeu173](https://doi.org/10.1093/ehjci/jeu173), indexed in Pubmed: [25240169](https://pubmed.ncbi.nlm.nih.gov/25240169/).
 19. Kataoka Yu, Hammadah M, Puri R, et al. Plaque vulnerability at non-culprit lesions in obese patients with coronary artery disease: Frequency-domain optical coherence tomography analysis. *Eur J Prev Cardiol*. 2015; 22(10): 1331–1339, doi: [10.1177/2047487315598711](https://doi.org/10.1177/2047487315598711), indexed in Pubmed: [26232281](https://pubmed.ncbi.nlm.nih.gov/26232281/).
 20. Lee SY, Shin DH, Shehata I, et al. Association between fractional flow reserve and coronary plaque characteristics assessed by optical coherence tomography. *J Cardiol*. 2016; 68(4): 342–345, doi: [10.1016/j.jcc.2015.10.012](https://doi.org/10.1016/j.jcc.2015.10.012), indexed in Pubmed: [26603326](https://pubmed.ncbi.nlm.nih.gov/26603326/).
 21. Kennedy MW, Fabris E, Ijsselmuiden AJ, et al. Combined optical coherence tomography morphologic and fractional flow reserve hemodynamic assessment of non-culprit lesions to better predict adverse event outcomes in diabetes mellitus patients: COMBINE (OCT-FFR) prospective study. Rationale and design. *Cardiovasc Diabetol*. 2016; 15(1): 144, doi: [10.1186/s12933-016-0464-8](https://doi.org/10.1186/s12933-016-0464-8), indexed in Pubmed: [27724869](https://pubmed.ncbi.nlm.nih.gov/27724869/).
 22. Moreno PR, Lodder RA, Purushothaman KR, et al. Detection of lipid pool, thin fibrous cap, and inflammatory cells in human aortic atherosclerotic plaques by near-infrared spectroscopy. *Circulation*. 2002; 105(8): 923–927, indexed in Pubmed: [11864919](https://pubmed.ncbi.nlm.nih.gov/11864919/).
 23. Madder RD, Smith JL, Dixon SR, et al. Composition of target lesions by near-infrared spectroscopy in patients with acute coronary syndrome versus stable angina. *Circ Cardiovasc Interv*. 2012; 5(1): 55–61, doi: [10.1161/CIRCINTERVENTIONS.111.963934](https://doi.org/10.1161/CIRCINTERVENTIONS.111.963934), indexed in Pubmed: [22253357](https://pubmed.ncbi.nlm.nih.gov/22253357/).
 24. Bourantas CV, Serruys PW, Nakatani S, et al. Bioresorbable vascular scaffold treatment induces the formation of neointimal cap that seals the underlying plaque without compromising the luminal dimensions: a concept based on serial optical coherence tomography data. *EuroIntervention*. 2015; 11(7): 746–756, doi: [10.4244/EIJY14M10_06](https://doi.org/10.4244/EIJY14M10_06), indexed in Pubmed: [25308301](https://pubmed.ncbi.nlm.nih.gov/25308301/).
 25. Komukai K, Kubo T, Kitabata H, et al. Effect of atorvastatin therapy on fibrous cap thickness in coronary atherosclerotic plaque as assessed by optical coherence tomography: the EASY-FIT study. *J Am Coll Cardiol*. 2014; 64(21): 2207–2217, doi: [10.1016/j.jacc.2014.08.045](https://doi.org/10.1016/j.jacc.2014.08.045), indexed in Pubmed: [25456755](https://pubmed.ncbi.nlm.nih.gov/25456755/).
 26. Kini AS, Baber U, Kovacic JC, et al. Changes in plaque lipid content after short-term intensive versus standard statin therapy: the YELLOW trial (reduction in yellow plaque by aggressive lipid-lowering therapy). *J Am Coll Cardiol*. 2013; 62(1): 21–29, doi: [10.1016/j.jacc.2013.03.058](https://doi.org/10.1016/j.jacc.2013.03.058), indexed in Pubmed: [23644090](https://pubmed.ncbi.nlm.nih.gov/23644090/).